Published in final edited form as:

Nat Metab. 2020 October ; 2(10): 1013–1020. doi:10.1038/s42255-020-0269-7.

Islet Transplantation in the Subcutaneous Space Achieves Long-term Euglycemia in Preclinical Models of Type 1 Diabetes

Ming Yu[1,*], **Divyansh Agarwal**[1,2,*,‡], **Laxminarayana Korutla**[1], **Catherine L. May**[3,4], **Wei Wang**[1], **Negin Noorchashm Griffith**[5], **Bernhard J. Hering**[6], **Klaus H. Kaestner**[3], **Omaida C. Velazquez**[7], **James F. Markmann**[8], **Prashanth Vallabhajosyula**[9], **Chengyang Liu**[1,‡], **Ali Naji**[1,3,‡]

[1]Division of Transplantation, Department of Surgery, Hospital of the University of Pennsylvania, Philadelphia, PA, 19104, USA.

[2]Medical Scientist Training Program, Genomics and Computational Biology, Perelman School of Medicine, University of Pennsylvania, Philadelphia, PA, 19104, USA.

[3]Institute for Diabetes, Obesity & Metabolism, Perelman School of Medicine, Philadelphia, University of Pennsylvania, Philadelphia, PA, 19104, USA.

[4]Department of Genetics, University of Pennsylvania, Philadelphia, PA, 19104, USA.

[5]Griffith Center for Restorative Surgery, Red Bank, NJ 07701, USA.

[6]Schulze Diabetes Institute, Department of Surgery, University of Minnesota, Minneapolis, MN, 55455, USA.

[7]Division of Vascular Surgery, DeWitt Daughtry Family Department of Surgery, University of Miami Miller School of Medicine, Miami, FL, 33136, USA.

[8]Division of Transplant Surgery, Massachusetts General Hospital, Harvard Medical School, Boston, MA, 02114, USA.

[9]Division of Cardiothoracic Surgery, Yale University School of Medicine, New Haven, CT, 06511, USA.

Abstract

‡Corresponding authors: Ali Naji, MD, PhD, Ali.Naji@uphs.upenn.edu, Ph: +01 (215) 817-5163, Chengyang Liu, MD, chliu@pennmedicine.upenn.edu, Ph: +01 (215) 200-5203, Divyansh Agarwal, PhD, divyansh.agarwal@pennmedicine.upenn.edu, Ph: +01 (267) 334-8324.

Author Contributions

A.N. conceptualized the study. O.C.V. provided the initial reagents that led to the development of an Islet Viability Matrix (IVM), and B.J.H. provided porcine islets. M.Y., N.N.G., C.L.M., C.L., D.A. and A.N. designed the transplantation and endocrine function experiments, conducted by M.Y., C.L.M., N.N.G., K.H.K., W.W., and C.L. Data analysis was led by D.A. Islet exosome research work was designed and conducted by L.K. and P.V.. D.A. and A.N. wrote the paper with feedback from all authors. J.F.M., C.L. and A.N. supervised the study.

*Co-first authors; these authors contributed equally to this work.

Competing Interests

The authors declare no competing interests

The intrahepatic milieu is inhospitable to intraportal islet allografts[1–3], limiting their applicability for the treatment of Type 1 Diabetes (T1D). Although the subcutaneous space represents an alternate, safe and easily accessible site for pancreatic islet transplantation, lack of neovascularization and the resulting hypoxic cell death have largely limited the longevity of graft survival and function, and pose a barrier for the widespread adoption of islet transplantation in the clinic. Here we report the successful subcutaneous transplantation of pancreatic islets admixed with a device-free Islet Viability Matrix (IVM), resulting in long-term euglycemia in diverse immune-competent and immuno-incompetent animal models. We validate sustained normoglycemia afforded by our transplantation methodology using murine, porcine and human pancreatic islets, and also demonstrate its efficacy in a nonhuman primate model of syngeneic islet transplantation. Transplantation of the islet–IVM mixture in the subcutaneous space represents a simple, safe and reproducible method, paving the way for a new therapeutic paradigm for T1D.

Pancreatic islet transplantation is the most effective β-cell replacement therapy to achieve precise glycemic control in patients with T1D.[4] Currently, clinical islet transplantation is based on intraportal infusion of pancreatic islets, which is fraught with complications, including hemorrhage, portal vein thrombosis, inflammatory response, and amyloidosis, ultimately resulting in graft loss.[1–3,5] Past attempts at utilizing alternative sites have been largely unsuccessful, necessitating surgical preparation of vascular beds, or dependent on a bioengineered module, with limited long-term follow-up (reviewed in[6]).[7–11] Interest in the subcutaneous space has garnered recent attention for transplantation of allogeneic stem cell-derived islets since it would facilitate monitoring for teratoma formation and allow simple complete excision of the graft if needed.[12,13] Yet, while the skin is a highly attractive site for islet transplantation owing to its safety profile and ease of access, paucity of nutrients and oxygen inevitably results in islet graft failure.[8,14,15]

The milieu in which islets are engrafted is critically important for their survival. Indeed, the importance of collagen 1 in the peri-islet extra-cellular environment in the healthy mammalian pancreas has been elucidated in past reports.[16,17] Building on this, attempts at restoring the peri-islet cytoarchitecture with oligomeric or encapsulation-based collagen matrices have demonstrated a pro-survival effect on mouse islet function both *in vitro* and *in vivo*.[8,18,19] Here, we report a previously undescribed mixture of human collagen 1, L-glutamine, fetal bovine serum, sodium bicarbonate and medium 199, which when admixed with murine, porcine or human islets, promotes uniform survival of the islets subcutaneously. The preparation of this compound, termed IVM, is described in Extended Data Fig. 1 (for a visual protocol, please see supplementary video 1).

In the immunoincompetent murine model, subcutaneous transplantation of 800 syngeneic islets without IVM into diabetic B6 SCID or WT B6 hosts uniformly failed to reverse diabetes, with most experiencing primary non-function (Fig. 1a). In contrast, even a 50% reduction in the islet mass, when bedaubed with IVM, consistently rendered the recipients normoglycemic within 24 hours post-transplantation (Fig. 1a). Excision of the islet-bearing skin invariably resulted in recurrence of diabetes. Histologic comparison of the tissue containing IVM-treated (IVM^+) versus control (IVM^-) islets demonstrated abundant healthy β-cells in the former cohort in contrast to loss of islet morphology and viability in the latter

(Extended Data Fig. 2). These observations were consistent across xenogeneic transplantation of porcine islets (Fig. 1a, Extended Data Fig. 2).

We next assessed whether human islets would experience similar survival when engrafted subcutaneously in diabetic immunoincompetent hosts. In contrast to human pancreatic islets transplanted without IVM, those engrafted with IVM uniformly reversed diabetes, corroborated by measurements of blood glucose (Fig. 1b) and human C-peptide (Fig. 1c). Excision of the islet-bearing skin in the long-term recipients of human islets led to prompt recurrence of hyperglycemia. The IVM^+ islets exhibited persistent collagen I in the islet extra-cellular environment and demonstrated preserved cellular morphology (Fig. 1d). Subsequently, we evaluated the kinetics of glucose disposal in recipients bearing long-term subcutaneous islets. Recipients bearing IVM^+ islets from mice, swine or humans (n=5 in each group) demonstrated normal glucose clearance, akin to healthy non-diabetic mice (Extended Data Fig. 3).

Having confirmed the efficacy of IVM in the absence of alloreactivity in immunoincompetent hosts, we sought to examine its potential in immune-competent rodent models. B6 recipients were placed on an immunosuppressive regimen (Fig. 2a, for details see Online Methods) targeting B and T cell compartments, with an anti-B lymphocyte stimulator (BLyS) antibody and rapamycin, respectively.[20] The animals were then subcutaneously transplanted with Balb/c islets (Fig. 2b), and histologic examination of the long-term euglycemic allografts demonstrated healthy and functional islets, and an absence of inflammatory or fibrotic reaction at the transplant site. A strong xenogeneic model, porcine-into-mouse, with the same immunosuppressive regimen recapitulated our findings, demonstrating preserved islet function even at post-operative day (POD) 51 in most of the recipients (Fig. 2b–c).

Next, we tested whether IVM might permit islet survival at other transplant sites, such as the retroperitoneal space. Indeed, either murine, porcine or human islets admixed with IVM and transplanted to the retroperitoneum uniformly restored normoglycemia across various species of diabetic mice (Fig. 3a). Similar to the subcutaneous grafts, excision of the retroperitoneal island containing pancreatic islets confirmed healthy cellular morphology and function (Fig. 3b). Collectively, these data confirm that IVM supports islet viability and insulin release *in vivo,* building on previous work where addition of extracellular matrix components such as collagen could induce islet adhesion and inhibit inflammation.[21–23] Additionally, we compared human islet graft survival with IVM in the subcutaneous space, with traditional islet transplant sites used in mice, *viz.,* the kidney capsule and portal vein, using a range of islet mass in genetically identical animals. The comparative analysis showed that the subcutaneous islet-IVM mixture consistently rendered the hosts normoglycemic at an earlier time post-transplantation (Extended Data Fig. 4).

To delineate whether IVM induces early changes in expression of the primary glucose receptor, Glut2 (SLC2A2), and insulin, we cultured human islets in the presence or absence of IVM and sampled a subset of the islets at days 0, 3 and 7. The expression of SLC2A2 and INSULIN were quantified at each time point between the IVM^+ and IVM^- islets. Although the SLC2A2 and INSULIN expression levels were initially similar in IVM^+ and IVM^- islets

in culture, at days 3 and 7 the IVM$^+$ group demonstrated significantly higher SLC2A2 levels (Extended Data Fig. 5a; $p<0.05$). Furthermore, while insulin expression levels fall sharply between days 3 and 7 in the IVM$^-$ islets, its levels were sustained and higher in the IVM$^+$ group, validating the improved functionality conferred by the IVM.

To further examine the kinetics of gene expression with islet endocrine function *in vivo*, we divided age-matched streptozotocin-treated NSG mice into two groups — in one group, human IVM$^+$ islets were subcutaneously engrafted, while the other group received IVM$^-$ islets. Glucose measurements at 3, 6, 24 and 48hr post-transplantation revealed that animals in the IVM$^+$ group achieve glucose homeostasis as early as 6hr post-engraftment (Fig. 4a). RNA analysis from human islet grafts excised at POD 2 from mice in both cohorts substantiated a significant increase in SLC2A2 expression ($p=0.002$) in recipients with an IVM$^+$ graft, and there was marked upregulation of SLC2A2, INSULIN and PDX1 (Fig. 4b). These insights, suggesting enhanced islet cell survival and replication in the presence of the islet-IVM mixture, were further supported by increased BrdU incorporation in the presence of IVM (Extended Data Fig. 5b–c).

Next, to probe the presence of a pro β-cell survival RNA signature in the IVM$^+$ population, we performed immunohistochemistry (IHC) on sections from the human-into-B6/SCID islet transplant model. Utilizing antibodies targeted at specific epitopes for Bcl-2, Von Willebrand Factor (VWF), vascular endothelial growth factor (VEGF) and glucagon-like peptide 1 (GLP-1), we observed that human IVM$^+$ islets had a significantly higher proportion and intensity for the stained epitopes compared to IVM$^-$ at POD 1 and 10 (Extended Data Fig. 6). The Bcl-2 family of proteins is important in inhibiting mitochondria-dependent extrinsic and intrinsic cell death pathways[24], whereas GLP-1 and GLP1R promote β-cell function and insulin secretion[25–27]. Therefore, we sought further evidence for whether an antiapoptotic mechanism might underlie the IVM-mediated success of subcutaneous islet transplantation using transplant islet-specific exosomes (TISEs) as a marker for the health status of the tissue[28].

Using human-into-mouse islet transplants, we compared intra-exosomal cargoes in recipients of IVM$^+$ and IVM$^-$ transplants at different time points during the first 10 days post-engraftment and found upregulation of markers associated with cellular regeneration and insulin regulation in the former. Specifically, anti-inflammatory and pro-cell survival were upregulated in islet exosomes from the IVM$^+$ group (Extended Data Fig. 7a–b). Furthermore, western blot analyses of circulating TISEs showed insulin expression almost exclusively in the IVM$^+$ exosomes, as well as an increase in GLP-1, GLP1R, Bcl-2 and Bcl-xL in the IVM$^+$ group compared to IVM$^-$ (Extended Data Fig. 7c). In accordance with the IHC and western blot data, further gene set analyses revealed upregulation of pro-angiogenic and proliferative pathways in the IVM$^+$ TISEs, whereas apoptosis and mTOR/MAPK/PI3K-Akt pathways were downregulated (Extended Data Fig. 7).

Lastly, in light of the translational potential of IVM, we developed a preclinical model of subcutaneous islet autotransplantation in a cynomolgus monkey (Fig. 4c; please see methods for details). After inducing diabetes through a ~90% pancreatectomy, autologous islets were transplanted subcutaneously. Grafting islets with IVM underneath the skin rendered the

monkey normoglycemic and a partial excisional biopsy at the transplantation site on POD 72 revealed preserved islet morphology, which was maintained even at POD 918 (Fig. 4c). The animal became insulin-dependent on POD 820, likely due to a concordant and progressive increase in body weight, or secondary to reduced islet mass due to a previous excisional skin biopsy. Moreover, at euthanasia, the monkey islets demonstrated robust viability and expressed Bcl-2, GLP-1 and VEGF (Extended Data Fig. 8), supporting the observations in rodent models that enhanced neovascularization, pro-survival signals, and downregulation of the apoptosome might contribute to islet survival subcutaneously in the presence of IVM.

In another cynomolgus monkey, following subtotal pancreatectomy the recipient was treated with streptozotocin to eliminate the native islets in the residual pancreatic head. The isolated islets were cultured overnight prior to subcutaneous transplantation with IVM the following day. During a year-long follow up, the animal remained diabetic, requiring daily insulin (Extended Data Fig. 9a). Biopsy of islet-bearing skin at POD 46 and 250 demonstrated healthy, insulin- and glucagon-positive islets at the transplant site, without peri-islet fibrosis or any mononuclear infiltration (Extended Data Fig. 9b). Despite the maintenance of islet morphology, this animal was not rendered euglycemic likely due to three factors (additional information detailing the clinical course of the animals is described in the methods). First, the islet yield from this monkey was significantly lower. Second, there was inevitable attrition of islets in culture. Third, streptozotocin may have led to β-cell glucotoxicity and subsequent loss of the transplanted islet cells *in vivo*, although the kinetics of streptozotocin have been previously studied in rodent models.[29] Nonetheless, these data collectively support the notion that IVM allows long-term persistence of islet viability subcutaneously, and that this protective effect appears to be mediated, at least in part, by an upregulation of anti-apoptotic signaling.

Subcutaneous pancreatic islet transplantation with IVM represents an impactful, translational alternative to intraportal islet delivery, the current clinical gold standard in T1D. Our data suggest that improved β-cell function in the presence of IVM could be mediated by the GLP1R signaling pathway, which has been found to upregulate the anti-apoptotic Bcl-2. GLP-1 also has glucoincretin and protective effects on β-cells, mediated in part by anti-oxidative effects.[25,26] By promoting sustained islet viability in the subcutaneous compartment, islets admixed with IVM maintain normal insulin and glucagon production. Establishment of this new method augments the utility of allogeneic pancreatic islet transplantation, future stem cell-derived and xenogeneic islet grafts, as well as related cellular therapies in tissue engineering and reparative medicine.[13]

METHODS

Composition and Preparation of the Islet Viability Matrix

Composition: 10x M199 (Sigma Life Science, Cat# M0650–100ML), L-glutamine (Mediatech Inc., Cat# 25–005-CI), FBS (HyClone Laboratories Inc., Cat# SH30071.03) 7.5% sodium bicarbonate, $NaHCO_3$ (Life Technologies Corporation, Cat# 25080–094), Type I collagen (Advanced BioMatrix, Cat# 5007–20ML)

Preparation: Extended Data Figure 1 shows the concentration of each ingredient to create one ml of IVM. Each ingredient and the final product must be kept on ice at all times to prevent solidification at higher temperatures. A tutorial for how to make the IVM is provided in supplementary video 1.

Murine Islet Transplantation Models

Animals: Immune competent (Balb/cByJ – Stock Number:000651, and C57BL/6J, B6 – Stock Number:000664), and Immune Incompetent (B6.Cg-Prkdc^{scid}/SzJ (B6/scid – Stock Number:001913), CBySmn.Cg-Prkdc^{scid}/J (Balb/c/scid – Stock Number:001803), NU/J (Balb/c/nude – Stock No: 002019), B6.Cg-Foxn1^{nu}/J (B6/nude – Stock Number:000819) and NOD-scid IL2Rgamma^{null} (NOG – Stock Number:005557)) male mice aged 8–12 weeks, used as islet donors and recipients, were obtained from the Jackson Laboratory, Bar Harbor, ME. Littermate controls were not utilized as these experiments involved transplantation of mouse, porcine and human islets into diabetic recipients.

Animals were housed in conditions to minimize stress, including a 12-hour light/12-hour dark cycle, ~50% humidity, and a 20–21°C temperature.

Diabetes Induction: Recipients were rendered diabetic by a single intraperitoneal injection of streptozotocin (SICOR Pharmaceuticals, Inc., Irvine, CA) at a dose of 200 mg/kg. At 5 days after streptozotocin (STZ) administration, animals with three consecutive (daily) non-fasting blood glucose levels >350 mg/dl (Contour Blood Glucose Monitoring System, Bayer HealthCare LLC, Mishawaka, IN, USA) were used as islet recipients. The protocol and all animal studies were approved by the Institutional Animal Care and Use Committee (IACUC) of The University of Pennsylvania (Protocol Numbers: 805662, 800932 and 805005), and in accordance with the Guide for the Care and Use of Laboratory Animals prepared by the U.S. National Institutes of Health.

Islet Isolation: Mouse pancreatic islet isolation was performed by collagenase P (Roche Diagnostics, Indianapolis, IN) digestion and density gradient separation.[1] Islets were maintained in a suspension of RPMI-1640 medium.

Islet Transplantation: The recipient mice were anesthetized by inhalation of 2–5 % Isoflurane (Isoflurane USP, Clipper Distribution Company LLC, St Joseph, MO, USA).

1. In the subcutaneous (SC) transplantation model, a small skin incision (0.3–0.5cm) was established over the lower abdomen to create a right and left lower quadrant SC pocket in which 400 fresh islets (hand-picked) were injected immediately in either a suspension of 360 μl of RPMI-1640 (“islets alone”; IA) or admixed in 360 μl IVM into right and left SC pockets separately.
2. In the retroperitoneal (RP) transplantation model, the mouse right lower abdominal cavity was opened, and 400 manually-picked fresh islets in either a suspension of 180 μl of RPMI-1640 (“islets alone”) or admixed in 180 μl IVM were injected with 25-gauge butterfly needle underneath the peritoneal layer in the right posterior retroperitoneal space.

Of note, regardless of the number of isolated islets (ranging from 200–800), the volume of IVM (360 μl IVM for SC and 180 μl IVM for RP) in which they were suspended remains the same, largely due to anatomical space constraints in the animal.

Immunosuppressive Regimen Following Allogeneic or Xenogeneic Transplantation in Mice: The immunosuppression regimen was based on targeting both T and B cells to promote the survival of islet allograft tolerance.[20] Briefly, the maintenance immunosuppression consisted of rapamycin (0.5 mg/kg intraperitoneal daily; qd), starting the day of islet transplantation for a duration of seven days. To target the B-cell compartment, we used 10F4, a monoclonal antibody against mouse B lymphocyte stimulator (BLyS), 100 μg intraperitoneally 20 days before transplant in two doses, 24 hours apart. 10F4 was provided by Human Genome Sciences, courtesy of Dr. Michael Cancro (Pathology and Laboratory Medicine, University of Pennsylvania), and eliminates primary B cells.[30] 10F4 was also given again starting day 10 in a tapering dose, from 50μg per week in week 2, down to 5μg per week starting week 8. The immunosuppression was discontinued at day 66.

Porcine Islet Transplantation Models

Islet Isolation: Porcine islets were obtained from Dr. Bernhard Herring's laboratory at the University of Minnesota. Islets were incubated in CMRL 1066 medium (Mediatech, Inc. Cat# 98–304-CV) containing 5.5 mm d-glucose, 0.05% human albumin (Telesis Biotherapeutics, Research Triangle Park, NC), 10 U/ml Heparin (Sagent Pharmaceuticals, Schaumberg, IL), 100 μg/ml penicillin/streptomycin, and 2 mM L-glutamine.

Islet Transplantation: The recipient mice were anesthetized by inhalation of 2–5 % Isoflurane (Isoflurane USP, Clipper Distribution Company LLC, St Joseph, MO, USA). The SC and RP transplantation experiments were carried out as detailed above in the "Murine Islet Transplantation Models" section. The protocol and all animal studies were approved by the Institutional Animal Care and Use Committee (IACUC) of The University of Pennsylvania (Protocol Numbers: 805662, 800932 and 805005), and in accordance with the Guide for the Care and Use of Laboratory Animals prepared by the U.S. National Institutes of Health.

Human Islet Transplantation Models

Islet Isolation: The comprehensive islet transplantation program at the University of Pennsylvania served as the resource for the human islets used in this study. Penn is part of the Integrated Islet Distribution Program (IIDP; https://iidp.coh.org/), and along with other centers, formed the Clinical Islet Transplant consortium (CIT) to initiate phase 3 trials of islet transplantation in Type 1 Diabetes. The source (either through IIDP or CIT) of the isolated human islets utilized in the experiments of the current manuscript were all procured according to the CIT manufacturing guidelines[31] which are described here: https://www.isletstudy.org. Human islets used via both the IIDP program as well as through CIT were procured at University of Pennsylvania's Islet GMP facility. Particularly with respect to the CIT, islets were obtained from pancreata that were originally intended for clinical use as part of the phase 3 clinical islet transplantation study.[4] However, from several donors, the

recovered yield was not high enough for clinical use despite high quality of the islets. These islet preps were then utilized for non-clinical activity such as distribution to research investigators and the experiments described in the current manuscript. We followed the release criteria as mandated by the NIH/FDA, including glucose-stimulated insulin release, restoration of normoglycemia in diabetic NOG mice, and perfusion studies for kinetics of insulin and glucagon secretion.

The recovery of pancreata from deceased organ donors was overseen under the auspices of the local/regional organ procurement agency (www.donors1.org; Gift of Life Donor Program, Philadelphia, PA, U.S.A.). The staff of the organ procurement agency obtained consent for organ recovery from the next of kin/donor's family members without any intervention from the investigators utilizing the organs for research, in accordance with the U.S. Federal Mandate. A summary of the characteristics of human islet donors used in our experiments is described in Extended Data Figure 10.

Islet Transplantation: The recipient mice were anesthetized by inhalation of 2–5 % Isoflurane (Isoflurane USP, Clipper Distribution Company LLC, St Joseph, MO, USA). The SC and RP transplantation experiments were carried out as detailed above in the "Murine Islet Transplantation Models" section.

Assessment of Islet Graft Function

Islet Graft Monitoring: Blood Glucose levels were monitored twice daily after transplantation and recipients with non-fasting glucose concentrations <200 mg/dL were considered to have achieved normoglycemia. When two consecutive daily non-fasting glucose levels were >300 mg/dl after a period of one week, islet grafts were considered to have failed and the recipient was considered to have primary non-function of the islet transplant.

Glucose Tolerance Test: An intraperitoneal glucose tolerance test (IPGTT) was performed on the animals with long-term normoglycemia (>100 days).[1] Blood glucose levels were analyzed using the Contour Blood Glucose Monitoring System (Bayer HealthCare LLC, Mishawaka, IN, USA).

Excision of Islet bearing site: In order to confirm that the islet grafts were the sole source of maintaining normoglycemia, a cohort of long term normoglycemic islet recipients, underwent excision of the islet bearing sites (skin or retroperitoneum). This uniformly led to prompt recurrence of diabetes within 24 hours. In recipients transplanted without IVM, the excision of the graft bearing site was carried out on day 7. In recipients transplanted with Islet+IVM the excision of the graft bearing site took place between 100–458 days.

Nonhuman Primate Models

Animals: Two male cynomolgus monkeys (*Macaca fascicularis*) were obtained from Spring Scientific Perkasie, PA, for autologous islet transplantation. Monkey 1 (ID #212077) had an initial body weight of 3.5 kg and age 4 years, whereas monkey 2 (ID #210069) had an initial body weight of 3.9kg and age 4 years. Prior to transplantation, serological testing

was performed on each animal to ensure that they were not infected with Herpes B, Schmidt-Ruppin strain of the Rous sarcoma virus, Simian T-cell Lymphotropic Virus (STLV), or Simian Immunodeficiency Virus (SIV). All animals had continuous water supply and were fed with regular primate diet supplemented with fresh fruits twice daily. All animal care and handling were performed in accordance with the guidelines established by the Department of Health and Human Services' guide for care and use of primates, as well as the IACUC guidelines.

Diabetes Induction: To perform islet auto-transplantation and assess the efficacy of IVM to promote islet engraftment in subcutaneous space in the absence of anti-islet alloreactivity, diabetes in the monkeys was induced by subtotal pancreatectomy (~85–90%) in 2 cynomolgus monkeys. Monkeys were sedated using ketamine (15mg/kg) and atropine (0.05mg/kg), prepared for operation, and intubated. Anesthesia was initiated with midazolam (1mg/kg) and maintained with isoflurane and oxygen. Haircoat was clipped closely from the nipples to mid-thigh and laterally to the end of the vertebral processes and skin, followed by scrubbing with a preliminary chlorhexidine solution. Animals were placed in a supine position, and the surgical field given a second chlorhexidine scrub. The abdomen was opened using a midline laparotomy. The spleen and greater omentum were reflected to expose the entire pancreas. The right and left pancreatic limbs were mobilized, preserving pancreatic vasculature, and the pancreas then carefully dissected from the duodenal serosa. The common pancreatic duct was identified at the duodenum, ligated, and transversely incised distal to the ligation. Through this incision, pancreatic duct was cannulated with an angio-catheter, and secured with ligature. The pancreas was then excised, placed in cold UW solution and transported to the islet isolation laboratory. Finally, the incisions were closed layer by layer. The animal was kept under general anesthesia while we processed the pancreas for islet isolation.

Islet Isolation: The islets were isolated by collagenase digestion and differential centrifugation.[32]

Subcutaneous Islet Transplantation: While under general anesthesia, the animals were placed in a supine position, and after the sterile prepping of the abdomen a small incision (3–4 cm) was established in left lower quadrant of the abdomen and the needle connected to a syringe containing the isolated islets plus IVM, was inserted into the subcutaneous space. The total volume of the inoculum was slowly infused in the subcutaneous compartment and the needle point was then swabbed with an antiseptic. Finally, the animal was recovered in an incubator and extubated thereafter. Per the advice of our IACUC veterinarians, we did not treat the monkeys with exocrine extracts during the post islet transplantation.

Islet graft function: According to IACUC recommendation, after transplantation the blood glucose levels in the islet auto-transplanted monkeys were monitored twice daily for the first three months, then daily thereafter. Recipients with non-fasting glucose concentrations <200 mg/dL were considered to have achieved normoglycemia requiring no daily exogenous insulin administration. When two consecutive daily non-fasting glucose

levels were >300 mg/dl after a period of primary graft function, islet grafts were considered to have failed mandating treatment with exogenous insulin twice daily. Towards POD 400, as a result of frequent blood sampling from the tip of the tail of animal, the tail developed a wound. The IACUC veterinarian's recommendation was to not sample the animal for a period of several weeks to months, giving it enough time to completely heal. Any gaps in daily blood glucose measurements during the 3-year-long follow up were based on the uniform recommendation of the veterinary staff to comply with ethical handling of the animal with proper care.

Biopsies of the islet bearing skin were performed under general anesthesia. Tissue samples (1–2 cm^2) were processed for standard H&E and IHC staining.

Tracking the clinical course of the cynomolgus monkeys: For cynomolgus monkey #212077 (body weight 3.5 kg), the excised pancreas weighed 6 grams, yielding 84,000 IEQs. The volume of the islet tissue pellet was 0.3ml which was added to 16.7ml of IVM yielding an inoculum containing 5,000 IEQ/ml of IVM. The entire inoculum (23,729 IEQ/kg body weight) was infused into the subcutaneous space. It is important to note that the pre-transplant glucose level in this monkey ranged from 30–110mg/dl. The duration from subtotal pancreatectomy to subcutaneous islet autotransplantation was 5 hours.

For cynomolgus monkey # 210069, in addition to the protocol detailed above, this animal received STZ (50mg/kg) after subtotal pancreatectomy to eliminate the residual native islets in the pancreatic head remnant. The excised pancreas weighed 5gm, yielding 46,125 IEQ's that were cultured in vitro overnight. During this period the monkey had free access to water and food and several blood glucose determinations revealed the level 200mg/dcl requiring exogenous insulin treatment. The islets were then removed from the culture. The volume of the islet tissue pellet was 0.2 ml which was added to 9.8 ml of IVM, yielding an inoculum containing about 5,000 IEQ/ml of IVM. The entire inoculum (11,827 IEQ/kg body weight) was transplanted subcutaneously into the LLQ of the abdomen. Of note, the duration from subtotal pancreatectomy to subcutaneous islet autotransplantation was 20 hours. In our attempts to eliminate the residual islets in the remnant of the pancreatic head, persistent STZ in the animal may have led to the loss of islet cells transplanted under the skin 20 hours after STZ administration.

BrdU incorporation assay

In vivo bromodeoxyuridine (BrdU) labeling was achieved by diluting drinking water with (1mg/ml) BrdU (Product # B9285, Sigma-Aldrich Co., LLC, St. Louis, MO) for 3 days, as described in[33]. Briefly, islet bearing skin sections containing human islets were harvested, fixed overnight with 4% paraformaldehyde, and processed for paraffin sectioning. Histological analysis of slides was performed using BrdU, Ki67, insulin, and glucagon. Slides were processed for immunostaining as follows: sections were incubated in blocking reagent (1% BSA in PBS) for 30 min, followed by incubation with the appropriate primary antibodies in the blocking reagent overnight at 4°C. Slides were washed thrice in PBS for 3–5 min each, followed by incubation for 45 min at room temperature in the appropriate secondary antibodies in blocking reagent. Slides were washed again in PBS (thrice for 5 min

each) and mounted. Images were captured on the Keyence All-in-One Fluorescence Microscope using the 0.95 NA 40X objective (Nikon). BrdU-positive nuclei were counted, blinded from at least 20 islet beta cells per mouse from four mice per group. The protocol was approved by the IACUC of the University of Pennsylvania.

RNA isolation for real-time (RT) PCR analysis

Islets from overnight fasted 18-wk-old mice were isolated using the standard collagenase procedure.[20] Islet purity was assessed by Dithizone staining and was determined to be >90% endocrine tissue. Total RNA from islets was isolated in Trizol (Invitrogen) followed by RNeasy mini kit or with RNeasy FFPE kit according to the Qiagen manufacturer's instructions. Islet RNA was reverse transcribed using either 1 μg of Oligo(dT) primer or random hexamer, SuperScript II Reverse Transcriptase, and accompanying reagents (Invitrogen). PCR reactions were assembled using the Brilliant SYBR Green QPCR Master Mix and performed using the SYBR Green (with Dissociation Curve) program on the Mx3005P qPCR System (Stratagene). All reactions were performed in triplicate with reference dye normalization, and median CT values were used for analysis. The primers used were as follows:

hSLC2A2 F: ATCCAAACTGGAAGGAACCC

hSLC2A2 R: CATGTGCCACACTCACACAA

hINSULIN F: AGGCCATCAAGCAGATCACT

hINSULIN R: GCACAGGTGTTGGTTCACAA

hPDX1 F: CCTTGTGCTCGGGTTATGTT

hPDX1 R: ATCATCCCACTGCCAGAAAG

hVEGF F: CTACCTCCACCATGCCAAGT

hVEGF R: GCAGTAGCTGCGCTGATAGA

Immunohistochemistry Analyses

Islet-bearing skin or native pancreatic tissue biopsy samples were fixed in Bouin's or formalin solution. The tissues were processed for routine histology and stained with hematoxylin and eosin (H&E). For immunohistochemical analysis, serial paraffin sections were prepared and stained using anti insulin and glucagon (DAKO Cytomation, Carpinteria, CA), anti-Bovine and human collagen I, anti-human Bcl-2, anti-human VWF, anti-human VEGF, anti-human GLP-1 (Abcam, Cambridge, MA) and anti-human Ki67 antibodies (ThermoScientific, Grand Island, NY). The anti-collagen antibodies were species specific with minimal to no cross-reactivity with mouse collagen. The following products were used: anti-human collagen antibody (Product # C-2456, Sigma, Saint Louis, US) and anti-bovine collagen antibody (NB100–64523, Novus Biologicals, US).

Immunofluorescence Antibodies conjugated with Cy2 or Cy3 IgG (Jackson IRL, West Grove, PA) were used as the second step reagents. Immunohistochemistry for Bcl-2, VWF, VEGF, GLP-1 staining was carried out using the Dako Envision+ system, peroxidase diaminobenzidine method (Dakocytomation, Carpinteria, CA). After de-paraffinization,

antigen retrieval was carried out by boiling the slides in 10mM citrate buffer, pH 6 or tris-based, pH 9 (Vector, Burlingame, CA) for 20 min. All antibodies at optimal dilution were incubated overnight at 4°C. Slides were then incubated with anti-rabbit or mouse HRP polymer for 30 min at room temperature followed by DAB+ substrate-chromagen solution for 5 min at room temperature. Slides were counterstained with hematoxylin and mounted. The details of all the antibodies used for immunohistochemistry are described in Supplementary Table 1.

The proportion and the intensity of the stained epitopes were evaluated using QuPath v0.1.2.[34] Prior to running the image analysis algorithm on a particular slide, automated image masking was performed per the developer's recommended steps (https://github.com/qupath/qupath/wiki). The accuracy of this automated ROI annotation was manually checked by an independent pathologist. Subsequently, QuPath's algorithm analyzed all ROIs in the inclusion annotation, excluding any tissue artifacts. Each section image had ≥ 5 ROIs of sufficiently high quality, and using each ROI as the unit of analysis, a Kruskal–Wallis H Test was performed to compare the output distributions for the proportion and intensity of staining between the IVM^+ and IVM^- groups.

Biochemical analysis of transplanted islet-specific exosome contents

Affinity antibody-coupled bead purification of tissue specific EVs.—MHC specific antibody was covalently conjugated to N-hydroxysuccinamide magnetic beads (Pierce) per manufacturer's protocol. 50 to 100 ug protein equivalent of EVs were incubated with antibody beads overnight at 4°C. The bead bound EV fractions were separated per manufacturer's protocol. EVs bound to beads were eluted using tris glycine and utilized for downstream analysis. Unconjugated HLA allele-specific anti-HLA A2 monoclonal IgG antibody (Catalogue # 0791HA) was purchased from One Lambda (West Hills, CA, USA), for donor HLA class I specific exosome isolation from recipient mouse plasma total pool of exosomes. Antibodies to insulin (15848–1-AP; used at a dilution of 1:200), TSG 101(28283–1-AP; used at a dilution of 1:500) were purchased from Proteintech Lab; antibodies to GLP1R (sc-390774; used at a dilution of 1:200), GLP-1(sc-57166; used at a dilution of 1:200), Bcl-2 (sc-7382; used at a dilution of 1:200), and Bcl-XL (sc-56021; used at a dilution of 1:200) were purchased from Santa Cruz Biotechnologies, Inc. Secondary antibodies conjugated to HRP (ready-to-use anti-rabbit, anti-mouse were purchased from Vector Lab: MP7451 and MP7452, respectively).

Extracellular vesicle (EV) isolation.—Exosomes were isolated from mouse plasma by using Sepharose 2B bead based size exclusion chromatography followed by ultracentrifugation.[28] Briefly, 250 ul to 500 ul of plasma was passed through a Sepharose 2B column. Eluent was collected in fractions and pooled after monitoring absorbance at 280 nm. The pooled fraction was ultracentrifuged at 110,000 g for 2 hours at 4°C, pellet was resuspended in 1XPBS for downstream analysis. Purified nanoparticles were analyzed on the NanoSight NS300 at light scatter mode for exosomes quantity and size distribution according to manufacturer's protocols (Malvern instruments Inc., MA, USA).

RNA isolation from exosomes.—Total RNA (including microRNAs and mRNA), was extracted from NHS-HLA-Class I bead bound exosomes using Trizol, followed by RNeasy mini kit, according to manufacturer's protocol (Qiagen, Germany).

Western blot analysis.—Donor HLA-class I specific exosomes bound to NHS-beads were lysed and separated on polyacrylamide gels, and transferred onto Nitrocellulose membrane (Life Technologies, NY, USA). The blot was blocked, incubated with desired primary antibody, HRP coupled secondary antibody (Santa Cruz Biotechnologies Inc.) per manufacturer's protocol and detected through Chemiluminescence using Phospho-Imager (Amersham Imager 680, GE Health, USA).

Library Preparation and Sequencing.—Exosomal RNA samples were assayed for quantity and quality with an Agilent 2100 Bioanalyzer instrument using the Agilent RNA 6000 Pico Kit (Agilent Technologies, Part number 5067–1513). Libraries were prepared using QIAseq miRNA Library Kit (QIAGEN, cat #331502) as per standard protocol in the kit's sample prep guide. Libraries were assayed for overall quality and quantified using High Sensitivity DNA Kit of Agilent 2100 Bioanalyzer (Agilent Technologies, Part number 5067–4626). Samples were multiplexed for sequencing. 100bp single-read sequencing of multiplexed pool of samples was carried out on an Illumina HiSeq 4000 sequencer. Illumina's bcl2fastq version v2.20.0.422 software was used to convert bcl to demultiplexed fastq files.

Trimming Adapter Sequence and UMI extraction.—The library prep kit when sequenced to 100bp produces reads a the read, a UMI, as well as fixed or nearly fixed sequences. We used the program cutadapt to remove the trailing adapter "AGATCGGAAGAGCACACGTCT" with settings -m 36 –max-n 1. We then extracted the UMI and the putative smRNA sequence using a custom R script. Briefly, we dropped trimmed reads that had more than 3 Ns, or were less than 55 bases long, or did not contain an exact match to the sequence "AACTGTAGGCACCATCAAT". The last 12 bases of reads were trimmed and recorded as the UMI. The 19 bases matching the inner adapter sequence were trimmed and the leading sequence was retained as the smRNA sequence. The UMI was appended to the def-line, and the trimmed read and base qualities were saved in FASTQ format.

Building chimeric bowtie libraries and transcript quantification.—We build three bowtie libraries (bowtie v1.2.3) that consisted of mouse and human (1) miRNA hairpins, (2) tRNAs, and (3) RefSeq sequences. The smRNA reads from above were aligned to each separately using the command 'bowtie -q -k 4 --best --sam --norc'. Expression of miRNA, tRNA, and RefSeq were quantified using the bowtie output files using a custom R script that used libraries 'Rsamtools', and 'GenomicAlignments' to process the bowtie BAM files. Simple species filtering and UMI reduction was performed as follows. Alignments were filtered to retain only those with the best bowtie stratum (XA BAM tag). Then any reads which had a top-stratum match to both human and mouse were discarded. UMI reduction was performed by binning unique combinations of reference sequence name (i.e., miRNA, tRNA, or RefSeq id), start position, and UMI. Overall raw expression for a reference

sequence was calculated as the number of unique reads aligning to each sequence. Raw read counts were also converted to CPM by adding a pseudocount of 1 to all detected transcripts, normalizing to total counts, then taking log2.

Statistics and Reproducibility

All statistical analyses were performed using R v3.5.3 (https://www.r-project.org). Data are expressed as mean ± standard deviation unless indicated otherwise. The significance of differences between two independent groups was calculated by the Wilcoxon Rank Sum/Mann-Whitney U Test, or the Student's two-sample *t-test*, as indicated in the figure legends. For representative IHC images, experiments were performed five independent times using distinct biological isolates. The IHC distributions obtained from QuPath were compared between the IVM^- and IVM^+ groups using the Kruskal–Wallis H Test. Cell culture experiments were repeated in independent biological triplicates to ensure reproducibility of the observations. Differences were considered significant at $P<0.05$ after Benjamini-Hochberg correction for multiple hypothesis testing. The initial pathway analyses were carried out using *multicross* (https://cran.r-project.org/web/packages/multicross/index.html)[35], and subsequent gene-set enrichment analysis performed using the WEB-based Gene SeT AnaLysis Toolkit (WebGestalt; http://www.webgestalt.org).[36] A filter of False Discovery Rate (FDR) < 0.05 was used to obtain selected pathways with the highest enrichment.

Unless stated otherwise in the legend, each experiment was repeated a minimum of five times per sample. Representative histology images shown in Figures 1d, 2c, 3b and 4c, as well as in the Extended Data Figures are chosen from among the best images available from the entire lot of technical replicates. Similar results were obtained each of the five times the histologic characterization of the grafts was done for each sample.

Data availability statement

Raw and processed exosome sequencing data have been submitted to GEO (Accession number GSE145593). Any additional information that supports the data within this paper and findings of this study are available from the corresponding authors upon request.

Extended Data

Ingredients	Concentration in 1ml IVM	Approximate Ratio
10x Medium (M) 199	91 µl	23
L-glutamine	8 µl	2
Fetal Bovine Serum (FBS)	100 µl	25
$NaHCO_3$ (7.5%)	23 µl	6
Type 1 Collagen	778 µl	195

Extended Data Figure 1: The constituents and their respective concentrations needed to create 1.0 mL of Islet Viability Matrix (IVM).
A visual protocol to make the IVM is described in supplementary video 1.

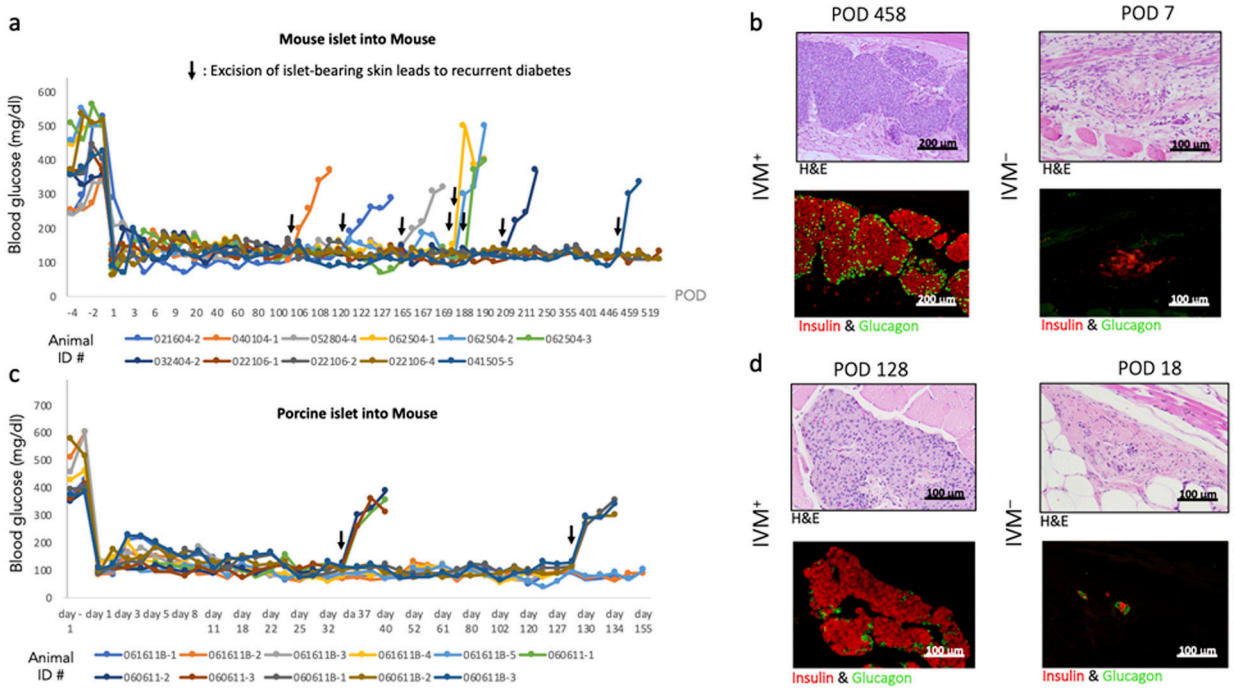

Extended Data Fig. 2: Syngeneic and xenogeneic islet transplantation in the subcutaneous space.

(a) and **(c)** Murine or porcine islet grafts were transplanted with IVM in immunoincompetent diabetic mice, following which non-fasting blood glucose level returned to physiological ranges (<200mg/dl) and remained stable long term. Hyperglycemia promptly resumed upon removal of the grafts (indicated by downward arrows in **(a)** and **(c)**). Additionally, we established the presence of viable and functional transplanted islets from donor mice **(b)** and pigs **(d)** in the subcutaneous space by histologic examination and staining for insulin (red) and glucagon (green).

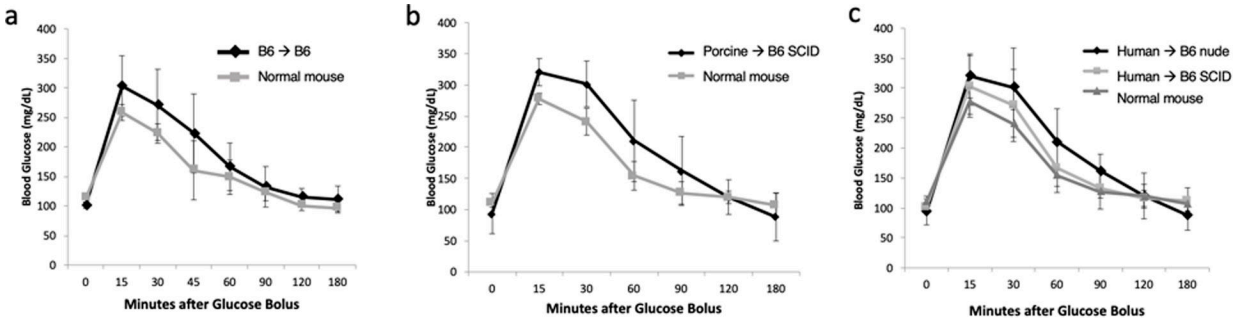

Extended Data Fig. 3: Intraperitoneal glucose tolerance test (GTT) in non-diabetic, normal/ healthy mice, compared with immunoincompetent mice with long term survival (>6 months) with subcutaneous islet-IVM grafts.

In each set of experiments, GTT kinetics were evaluated in controls (n = 5) and B6 recipients of **(a)** mouse islets (n = 5) and **(b)** porcine islets (n = 5). GTT was also performed in B6 nude and B6 SCID recipients of **(c)** human islets (n=5 in each group). Islet grafts in the subcutaneous tissue promptly restore normoglycemia upon glucose challenge. Mean glycemic values for each experimental group are plotted, and the error bars represent the

standard deviation. There were no statistically significant differences in glucose regulation between healthy/normal mice and the IVM^{+} islet transplant groups.

Recipient	N/sample size	Number of Islets	Transplant Site*	Graft$^{\gamma}$	NG_{24}	NG_{48}	NG_{168}
NSG	8	200	KC	IA	0	0	25
NSG	6	200	PV	IA	0	0	17
NSG	6	200	SC	IVM	17	33	67
NSG	10	400	KC	IA	60	60	80
NSG	6	400	PV	IA	33	50	67
NSG	8	400	SC	IVM	88	100	100
B6/Nude	10	500	KC	IA	60	70	100
B6/Nude	5	500	PV	IA	60	60	80
B6/Nude	10	500	SC	IVM	80	80	100

*KC = Kidney Capsule; PV = Portal Vein; SC = Subcutaneous Space.
$^{\gamma}$ IA = islets alone; IVM = islets implanted subcutaneously with IVM.
NG_x = % of animals normoglycemic within *x* hours
NSG = non-obese diabetic SCID gamma mouse

Extended Data Figure 4: Table comparing the human islet graft survival with IVM in the subcutaneous space, with traditional islet transplant sites used in mice, viz., the kidney capsule and portal vein.

Of note, the same protocol for islet isolation and preparation was followed and N animals were used to for each particular set of transplant experiments. Hand-picked, healthy human islets transplanted in the subcutaneous space with IVM uniformly resulted in normoglycemia, whereas the same number of islets transplanted in the kidney capsule and the portal vein in the genetically identical animals resulted in a delayed restoration of normoglycemia.

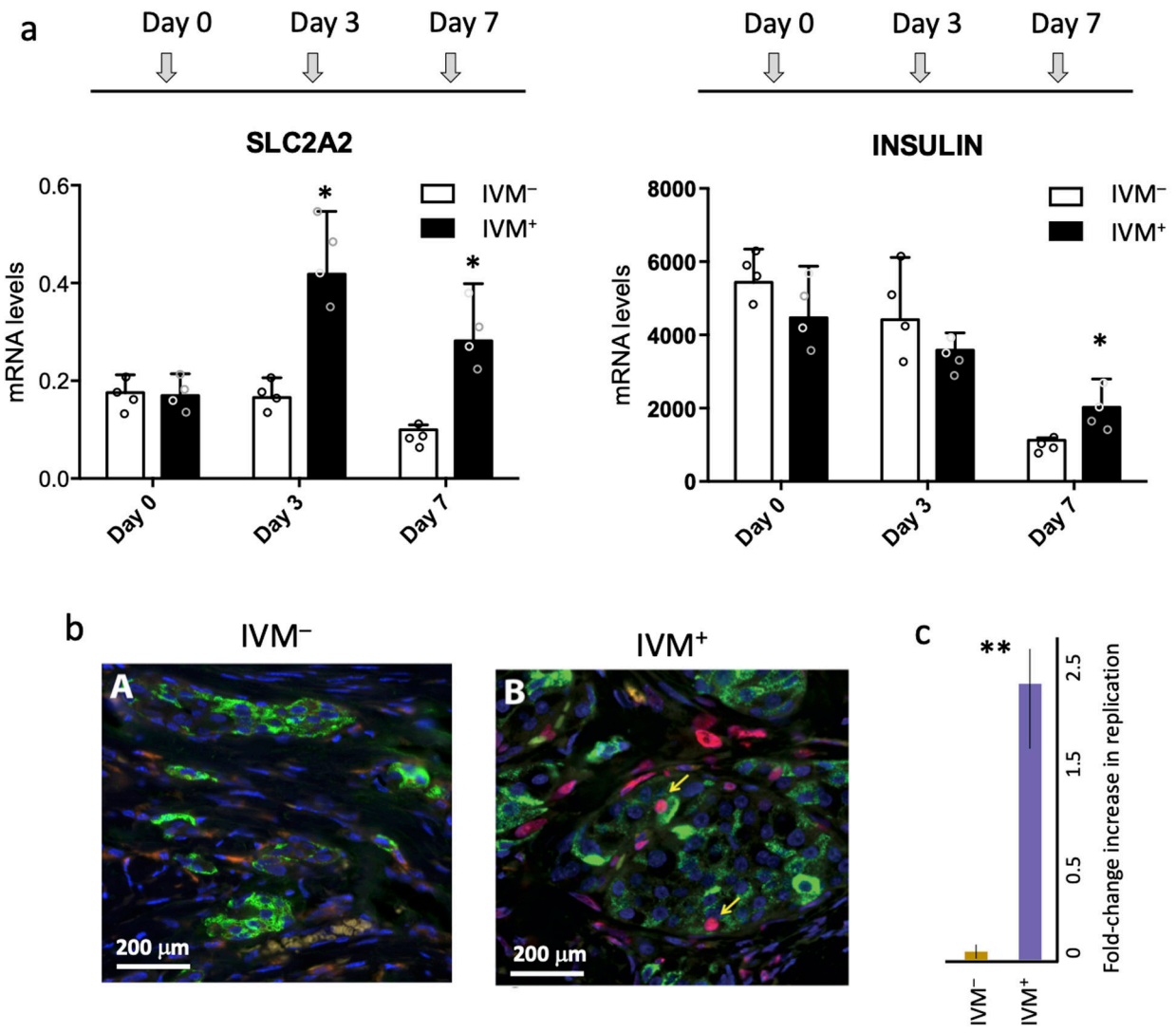

Extended Data Fig. 5: SLC2A2 (Glut2) and INSULIN levels were upregulated at day 7 in islet culture with IVM (n=4 animals in each group).

(a) All gene expressions were normalized to TBP and expressed as mean ± SEM. * denotes $p < 0.05$ based on a one-sided Student's t-test. Each dot represents an individual data point. No p-value correction for multiple hypothesis adjustment was done. The p-values corresponding to SLC2A2 at days 3 and 7 were 0.006 and 0.01 respectively; p=0.008 for INSULIN at day 7. **(b)** Human islets transplanted subcutaneously in immune-incompetent diabetic mice with and without IVM (n=4 mice in both groups) were excised on POD7, and the grafts were immunoassayed for insulin (green), BrdU (red) and counterstained for nuclear DNA with DAPI (blue). Yellow arrows point to β-cells with DNA replication as indicated by BrdU incorporation. One hundred insulin$^+$ cells were counted per section in the IVM$^+$ group, whereas <20 insulin$^+$ cells could be counted in the IVM$^-$ cohort. The red structures represent nuclei, albeit some nuclei appear *en face* or out of plane**. (c)** Quantification of DNA replication rate in IVM$^+$ and IVM$^-$ cohorts (n=100 cells in the IVM+ group and 18 cells in the IVM$^-$ group) shows increased replication in the IVM$^+$ group (** indicates one-sided Student's t-test $p=4\times10^{-5}$).

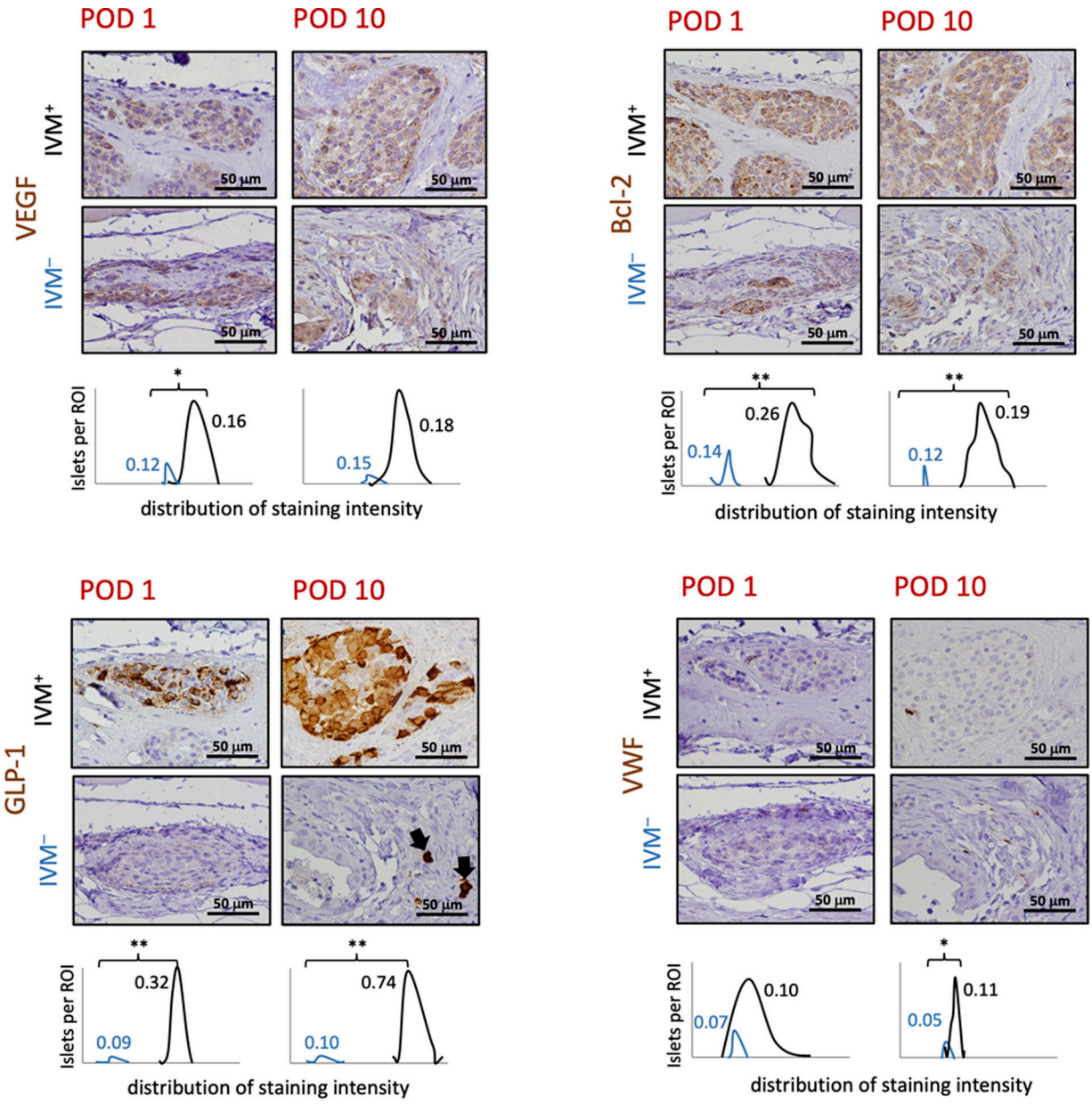

Extended Data Fig. 6: Based on human-into-mouse islet transplant model, immunohistochemical profiling of islets ± IVM for markers of angiogenesis (VEGF), anti-apoptosis (Bcl-2, GLP-1) and endothelial cells (VWF) highlights the increased intensity and stained area of these epitopes in the IVM$^+$ group.

The proportion and intensity of staining, quantified by QuPath using five automated regions of interest (ROIs) per sectioned image, is plotted below each section (* denotes $p < 0.05$ and ** denotes $p < 5\times10^{-5}$ based on the one-way Kruskal–Wallis H Test; arrow in the GLP-1 IVM$^-$ section denotes staining artifact). The particular significant p-values were — VEGF at POD 1 (p=0.009), Bcl-2 at POD1 (p=7×10^{-8}) and POD10 (p=10^{-9}), GLP-1 at POD1 (p=10^{-8}) and POD 10 (p=4×10^{-9}) and VWF at POD 10 (p=2×10^{-4}).

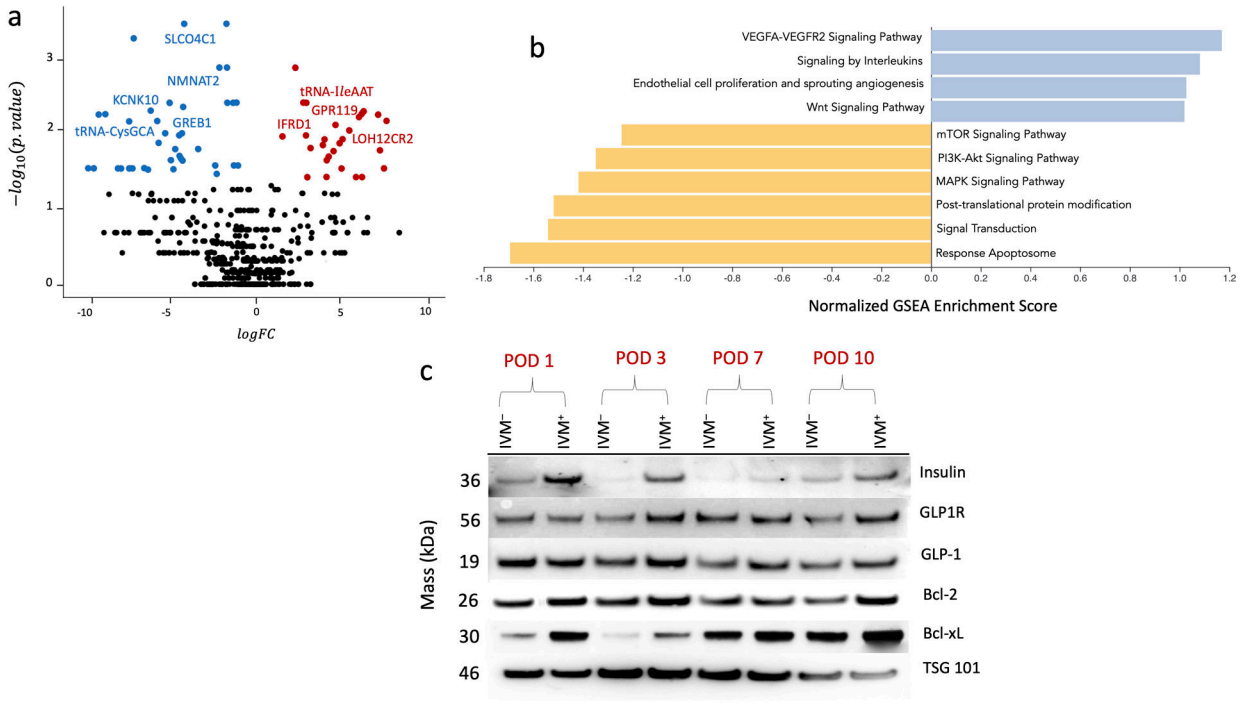

Extended Data Fig. 7: Circulating human TISEs isolated at 6hr, 12hr, and on PODs 1, 3 and 10 from the IVM$^+$ and IVM$^-$ cohorts were sequenced.

Differential expression across the five time points analyzed using one-sided Mann-Whitney U, as summarized in the Volcano Plot **(a)**. The *x*-axis is $\log_2$ ratio of gene expression levels between the two cohorts; the *y*-axis is the Benjamin Hochberg-adjusted p-value based on $-\log_{10}$. The colored dots represent the differentially expressed genes (blue = lower expression; red = higher expression in the IVM$^+$ cohort) based on $p<0.05$ and two-fold expression difference. Gene Set Enrichment Analysis identified the major pathways (FDR ≤ 0.05) that were either upregulated or downregulated in the IVM$^+$ group **(b)**. TISEs from IVM$^+$ group showed higher expression of β-cell-specific proteins and anti-apoptotic markers as part of its intraexosomal cargo by Western blot analysis **(c)**. TSG101 protein is shown as a canonical exosome marker.

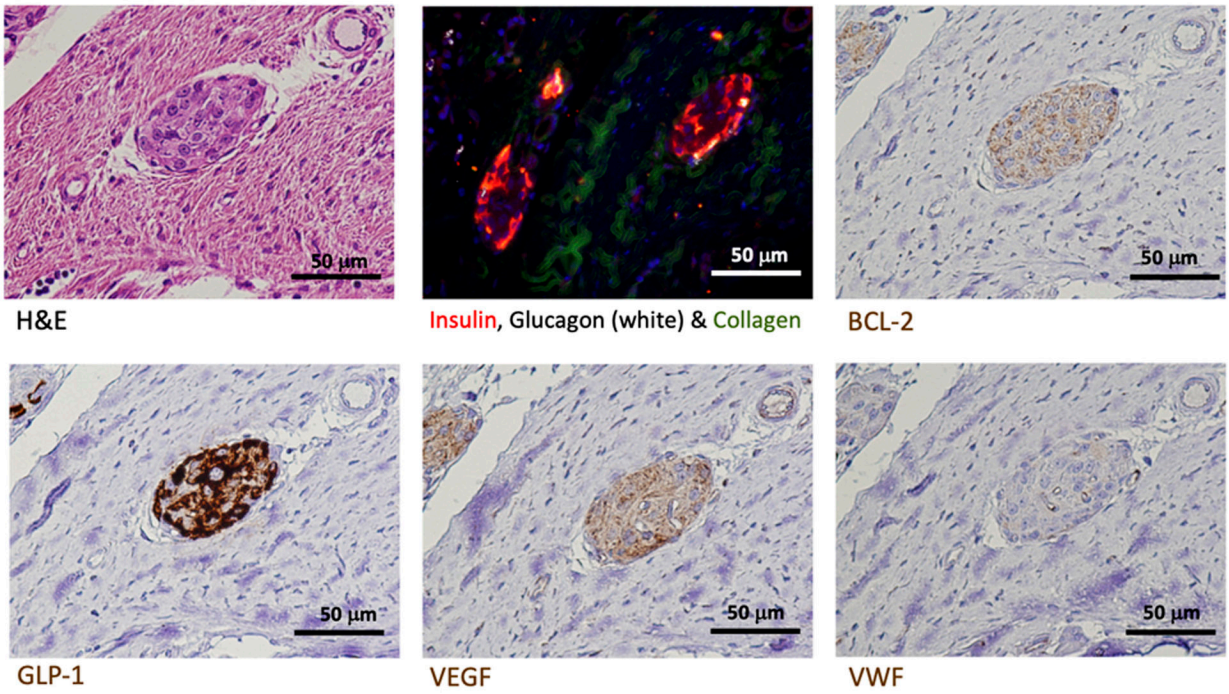

Extended Data Fig. 8: Morphological and immunohistochemical analysis of autologous cynomolgus monkey islets, implanted in the subcutaneous space, was performed at the time of euthanasia (animal ID# 212077, POD 918).

We found abundant healthy islet cell clusters, exhibiting vivid expression of key markers such as Insulin, Glucagon, Bcl-2, GLP-1, Ki67, VEGF, VWF and Collagen. Due to IACUC regulations and ethical care guidelines for nonhuman primate research, subcutaneous autologous islet transplants without IVM as a control could not be performed in a cynomolgus monkey.

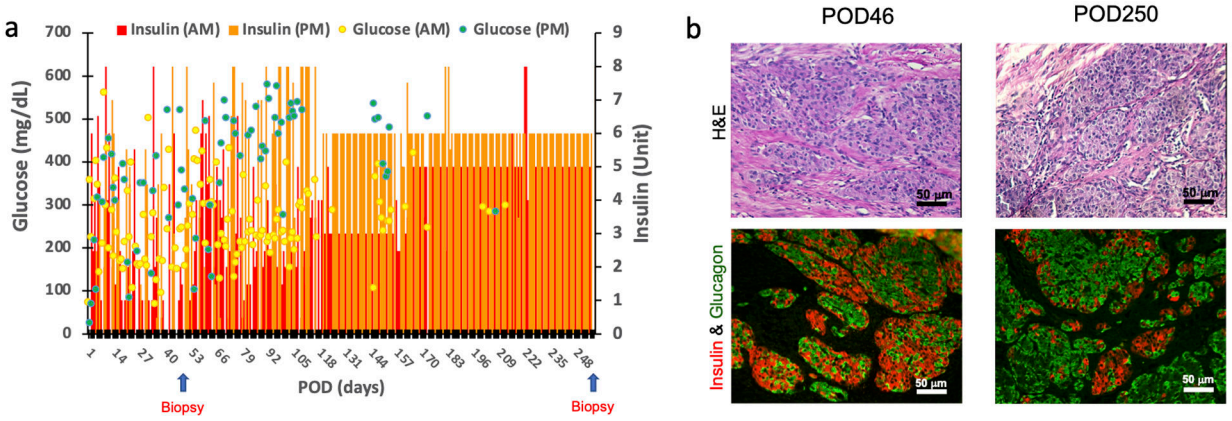

Extended Data Fig. 9: For cynomolgus monkey ID# 210069, the animal's blood glucose just prior to pancreatectomy was 72 mg/dl; blood glucose monitoring post-transplantation demonstrated persistent hyperglycemia in the animal, which required management by exogenous insulin therapy.

(a) Failure to achieve normoglycemia in this monkey can be attributed partly to the suboptimal islet yield and transplantation of a relatively low mass of islets (11,827 IEQs/kg

body weight), as well as the infusion of streptozotocin which likely led to the destruction of both native remnant islets as well as subcutaneously transplanted islets. **(b)** In view of the persistent state of insulin dependency and per the recommendation of the IACUC veterinarian, the monkey was subjected to euthanasia on POD 250. During this course, an excisional biopsy of the islet bearing skin was performed on POD 46 and at the time of euthanasia. Both histologic assessments revealed abundant well granulated islet β-cells as well as glucagon-positive α-cells

Donor age (years)	Gender	Islet Characteristics				Experiments*
		Purity	Viability	GSIR$^{\gamma}$	DNA content per islet (ng)	
42	M	90	88	2.1	4.5	Fig. 1
53	F	90	91	1.4	10.1	Fig. 1
56	M	90	91	1.2	2.4	Fig. 1
40	M	90	89	1.1	2.3	Fig. 1
51	M	95	77	1.3	8	Fig. 1
51	M	90	73	1.4	4.2	Fig. 1
50	F	90	93	1	13.4	Fig. 1
53	M	90	88	1.05	2.5	Fig. 1
19	M	70	95	1.19	4.8	Fig. 1
15	M	75	93	1.1	3.2	Fig. 1
50	F	85	96	2.8	4.2	Fig. 1
51	F	90	96	1.63	2.6	Fig. 1
16	M	70	91	3.53	4.4	Fig. 1,3
51	F	80	94	2.8	6.1	Fig. 1,3
39	F	96	94	1.31	3.4	Fig. 1,3
24	M	90	92	0.6	5.2	Figs. 1, 4
13	M	95	91	0.78	4.5	Figs. 1, 4
35	M	90	94	1.16	5.2	Figs. 1, 4
55	M	85	91	1.8	1.8	Figs. 1, 4
40	M	80	93	2.4	1.3	ED Figs. 2-5
44	F	90	95	1.6	1.4	ED Figs. 2-5
17	F	80	94	3.3	1.24	ED Figs. 2-5
35	F	85	94	1.9	6.9	ED Figs. 2-5
20	M	80	92	1.6	2.24	ED Figs. 2-5
41	F	90	97	2.55	7.3	ED Table 1
29	M	90	93	2	5.5	ED Table 1
21	M	90	95	1.5	1.9	ED Table 1

$^{\gamma}$GSIR = Glucose-Stimulated Insulin Release *ED = Extended Data

Extended Data Figure 10:
Characteristics of human islet donors used in the described experiments

Supplementary Material

Refer to Web version on PubMed Central for supplementary material.

Acknowledgements

We wish to thank S. Rostami, B. Koeberlein and G. Quinn for their valuable assistance in data collection and development of animal models. We are grateful to Y.J. Wang for helping with the islet beta cell BrdU staining experiments. We also acknowledge the support of J. Schug, Technical Director of the Next-Generation Sequencing Core at the University of Pennsylvania, in the exosome sequencing analysis. We are grateful to the members of the pancreatic islet isolation team at the University of Pennsylvania - Y. Li, Z. Min and X. Zuo. D.A. would like to thank the Blavatnik Family Foundation Graduate Student Fellowship he received during his MD/PhD training. We would also like to thank the National Institutes of Health for the award, NIH/NIDDK DK070430, NIH/NIAID AI-102430, NIH/NIDDK UC4-112217 (HPAP), and the NIDDK Integrated Islet Distribution Program (IIDP) Grant (Beckman Research Center #10028044), awarded to A.N.

References:

1. Kawahara T et al. Portal vein thrombosis is a potentially preventable complication in clinical islet transplantation. Am. J. Transplant 11, 2700–2707 (2011). [PubMed: 21883914]
2. Moberg L et al. Production of tissue factor by pancreatic islet cells as a trigger of detrimental thrombotic reactions in clinical islet transplantation. Lancet 360, 2039–2045 (2002). [PubMed: 12504401]
3. Walsh TJ, Eggleston JC & Cameron JL Portal hypertension, hepatic infarction, and liver failure complicating pancreatic islet autotransplantation. Surgery 91, 485–487 (1982). [PubMed: 6801798]
4. Hering BJ et al. Phase 3 Trial of Transplantation of Human Islets in Type 1 Diabetes Complicated by Severe Hypoglycemia. Diabetes Care 39, 1230–1240 (2016). [PubMed: 27208344]
5. Ricordi C & Strom TB Clinical islet transplantation: advances and immunological challenges. Nat. Rev. Immunol 4, 259–268 (2004). [PubMed: 15057784]
6. Smink AM, Faas MM & de Vos P Toward engineering a novel transplantation site for human pancreatic islets. Diabetes 62, 1357–1364 (2013). [PubMed: 23613549]
7. Ao Z, Matayoshi K, Lakey JR, Rajotte RV & Warnock GL Survival and function of purified islets in the omental pouch site of outbred dogs. Transplantation 56, 524–529 (1993). [PubMed: 8212144]
8. Vlahos AE, Cober N & Sefton MV Modular tissue engineering for the vascularization of subcutaneously transplanted pancreatic islets. Proc. Natl. Acad. Sci. U. S. A 114, 9337–9342 (2017). [PubMed: 28814629]
9. Pepper AR et al. A prevascularized subcutaneous device-less site for islet and cellular transplantation. Nat. Biotechnol 33, 518–523 (2015). [PubMed: 25893782]
10. Cantarelli E et al. Bone marrow as an alternative site for islet transplantation. Blood 114, 4566–4574 (2009). [PubMed: 19773545]
11. Pepper AR et al. Long-term function and optimization of mouse and human islet transplantation in the subcutaneous device-less site. Islets 8, 186–194 (2016). [PubMed: 27820660]
12. Pepper AR et al. Transplantation of Human Pancreatic Endoderm Cells Reverses Diabetes Post Transplantation in a Prevascularized Subcutaneous Site. Stem Cell Rep. 8, 1689–1700 (2017).
13. Odorico J et al. Report of the Key Opinion Leaders Meeting on Stem Cell-derived Beta Cells. Transplantation 102, 1223–1229 (2018). [PubMed: 29781950]
14. Juang J-H, Hsu BR-S & Kuo C-H Islet transplantation at subcutaneous and intramuscular sites. Transplant. Proc 37, 3479–3481 (2005). [PubMed: 16298634]
15. Lacy PE, Hegre OD, Gerasimidi-Vazeou A, Gentile FT & Dionne KE Maintenance of normoglycemia in diabetic mice by subcutaneous xenografts of encapsulated islets. Science 254, 1782–1784 (1991). [PubMed: 1763328]
16. Smink AM & de Vos P Therapeutic Strategies for Modulating the Extracellular Matrix to Improve Pancreatic Islet Function and Survival After Transplantation. Curr. Diab. Rep 18, 39 (2018). [PubMed: 29779190]

17. Van Deijnen JH, Van Suylichem PT, Wolters GH & Van Schilfgaarde R Distribution of collagens type I, type III and type V in the pancreas of rat, dog, pig and man. Cell Tissue Res. 277, 115–121 (1994). [PubMed: 8055531]
18. Vlahos AE et al. Endothelialized collagen based pseudo-islets enables tuneable subcutaneous diabetes therapy. Biomaterials 232, 119710 (2020). [PubMed: 31901691]
19. Stephens CH et al. In situ type I oligomeric collagen macroencapsulation promotes islet longevity and function in vitro and in vivo. Am. J. Physiol.-Endocrinol. Metab 315, E650–E661 (2018). [PubMed: 29894201]
20. Parsons RF et al. Murine islet allograft tolerance upon blockade of the B-lymphocyte stimulator, BLyS/BAFF. Transplantation 93, 676–685 (2012). [PubMed: 22262127]
21. Lucas-Clerc C, Massart C, Campion JP, Launois B & Nicol M Long-term culture of human pancreatic islets in an extracellular matrix: morphological and metabolic effects. Mol. Cell. Endocrinol 94, 9–20 (1993). [PubMed: 8375579]
22. Weber LM & Anseth KS Hydrogel encapsulation environments functionalized with extracellular matrix interactions increase islet insulin secretion. Matrix Biol. J. Int. Soc. Matrix Biol 27, 667–673 (2008).
23. Jiang K et al. 3-D physiomimetic extracellular matrix hydrogels provide a supportive microenvironment for rodent and human islet culture. Biomaterials 198, 37–48 (2019). [PubMed: 30224090]
24. Kale J, Osterlund EJ & Andrews DW BCL-2 family proteins: changing partners in the dance towards death. Cell Death Differ. 25, 65–80 (2018). [PubMed: 29149100]
25. Portha B, Tourrel-Cuzin C & Movassat J Activation of the GLP-1 receptor signalling pathway: a relevant strategy to repair a deficient beta-cell mass. Exp. Diabetes Res 2011, 376509 (2011). [PubMed: 21716694]
26. Xiong X, Shao W & Jin T New insight into the mechanisms underlying the function of the incretin hormone glucagon-like peptide-1 in pancreatic β-cells: the involvement of the Wnt signaling pathway effector β-catenin. Islets 4, 359–365 (2012). [PubMed: 23314611]
27. Tomas A, Jones B & Leech C New Insights into Beta-Cell GLP-1 Receptor and cAMP Signaling. J. Mol. Biol 432, 1347–1366 (2020). [PubMed: 31446075]
28. Vallabhajosyula P et al. Tissue-specific exosome biomarkers for noninvasively monitoring immunologic rejection of transplanted tissue. J. Clin. Invest 127, 1375–1391 (2017). [PubMed: 28319051]
29. Wu J & Yan L-J Streptozotocin-induced type 1 diabetes in rodents as a model for studying mitochondrial mechanisms of diabetic β cell glucotoxicity. Diabetes Metab. Syndr. Obes. Targets Ther 8, 181–188 (2015).
30. Scholz JL et al. BLyS inhibition eliminates primary B cells but leaves natural and acquired humoral immunity intact. Proc. Natl. Acad. Sci. U. S. A 105, 15517–15522 (2008). [PubMed: 18832171]
31. Ricordi C et al. National Institutes of Health-Sponsored Clinical Islet Transplantation Consortium Phase 3 Trial: Manufacture of a Complex Cellular Product at Eight Processing Facilities. Diabetes 65, 3418–3428 (2016). [PubMed: 27465220]
32. Liu C et al. B lymphocyte-directed immunotherapy promotes long-term islet allograft survival in nonhuman primates. Nat. Med 13, 1295–1298 (2007). [PubMed: 17965721]
33. Avrahami D et al. Targeting the cell cycle inhibitor p57Kip2 promotes adult human β cell replication. J. Clin. Invest 124, 670–674 (2014). [PubMed: 24430183]
34. Bankhead P et al. QuPath: Open source software for digital pathology image analysis. Sci. Rep 7, 16878 (2017). [PubMed: 29203879]
35. Agarwal D, Mukherjee S, Bhattacharya BB & Zhang NR Distribution-Free Multisample Test Based on Optimal Matching with Applications to Single Cell Genomics. ArXiv190604776 Stat (2019).
36. Wang J, Vasaikar S, Shi Z, Greer M & Zhang B WebGestalt 2017: a more comprehensive, powerful, flexible and interactive gene set enrichment analysis toolkit. Nucleic Acids Res. 45, W130–W137 (2017). [PubMed: 28472511]

a

Donor	Recipient	Number of islets	Graft	Islet graft survival in days (number of mice)
B6	B6/SCID	800	IA	Primary non-function ($n = 8$)
B6	B6/SCID	800	Islets + IVM	127(×2), 115(×2), 112(×2)
B6	B6	800	IA	Primary non-function ($n = 12$)
B6	B6	800	Islets + IVM	529(×3), 458, 209(×2), 186(×3), 165(×2)
B6	B6/SCID	400	IA	Primary non-function ($n = 6$)
B6	B6/SCID	400	Islets + IVM	227 (×2), 165 (×2), 120, 106, 104 (×2)
B6	B6	400	IA	Primary non-function ($n = 6$)
B6	B6	400	Islets + IVM	504 (×3), 463 (×3), 457 (×2), 292(×5), 247(×3)
Porcine	Balb/c/nude	500	IA	Primary non-function ($n = 6$)
Porcine	Balb/c/nude	500	Islets + IVM	56 (×2), 49 (×2)
Porcine	Balb/c/SCID	500	IA	Primary non-function ($n = 6$)
Porcine	Balb/c/SCID	500	Islets + IVM	155 (×3), 127 (×2), 124, 82(×2), 81
Porcine	B6/SCID	500	IA	Primary non-function ($n = 4$)
Porcine	B6/SCID	500	Islets + IVM	160,128 (×3), 36 (×3)
Porcine	B6/SCID	250	Islets + IVM	125(×5)
Porcine	NOG	500	IA	Primary non-function ($n = 6$)
Porcine	NOG	500	Islets + IVM	177(×3), 136(×4)
Human	B6/nude	400	IA	Primary non-function ($n = 4$)
Human	B6/nude	400	Islets + IVM	238, 231(×2), 128 (×2), 99, 61 (×2)
Human	B6/SCID	400	IA	Primary non-function ($n = 8$)
Human	B6/SCID	400	Islets + IVM	192 (×2), 121 (×2), 99 (×2), 95 (×2), 78(×2), 49

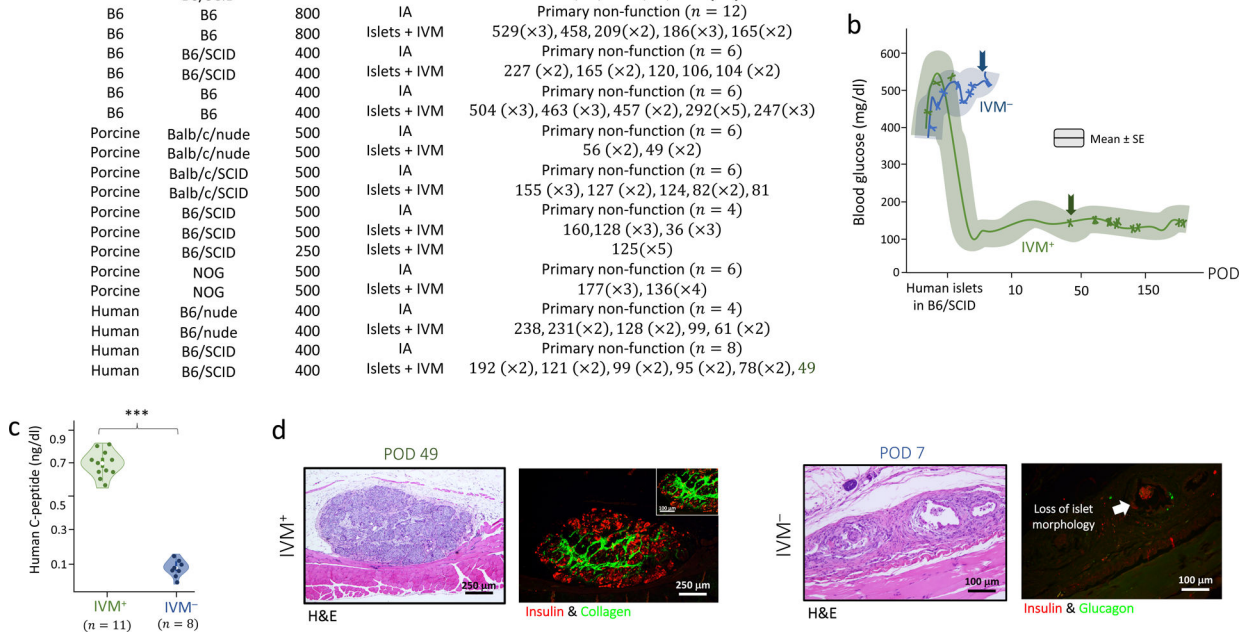

Figure 1.

Pancreatic islets transplanted in the subcutaneous space with IVM promote optimal glucose homeostasis in immunoincompetent diabetic hosts. **(a)** Either murine, porcine or human islets were admixed with or without IVM and grafted subcutaneously. Individual islet graft survival across different animal models is summarized. Islets transplanted without IVM uniformly resulted in primary non-function. In all cases, the days in the IVM^+ group represent excision of the islet bearing skin at the times of elective retrieval and not due to destabilization of the grafts. **(b)** Metabolic homeostasis evaluated by glucose measurements in B6/SCID animals transplanted with human islets ± IVM showed that IVM^+ islets consistently rendered the recipients normoglycemic. **(c)** Human C-peptide levels were measured in the serum of theses recipients and are shown in the violin plot. Each dot represents the C-peptide measured from an individual recipient mouse. Difference in C-peptide levels was statistically significant (*** denotes $p<10^{-5}$ based on the one-sided Mann-Whitney U Test). **(d)** As a representative example, in B6/SCID mice, at POD7 in the IVM^- cohort and POD49 in the IVM^+ cohort an excisional biopsy was performed, showcasing fragmented $Insulin^+$ cells in the former group, in contrast to preserved islet architecture and integrated collagen in the latter.

a

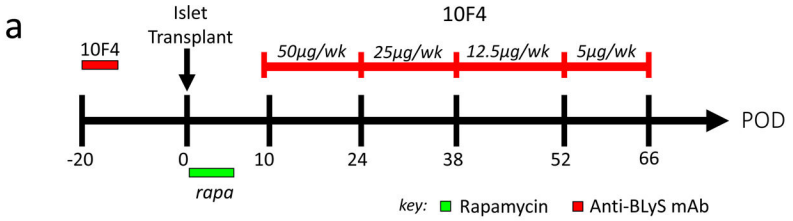

b

Donor	Recipient	Number of islets	Graft	Immunosuppression	Islet graft survival in days (number of mice)
Balb/c	B6	400	IA	–	Primary non-function ($n = 6$)
Balb/c	B6	400	Islets + IVM	Rapamycin	$23^{\phi}(\times 2), 13^{\phi}(\times 2), 11^{\phi}(\times 2)$
Balb/c	B6	400	Islets + IVM	Rapamycin + anti-BLyS	$707(\times 2), 185(\times 2), 111, 90$
Porcine	B6	400	IA	–	Primary non-function ($n = 4$)
Porcine	B6	400	Islets + IVM	Rapamycin + anti-BLyS	$51(\times 3), 7^{\phi}(\times 2)$

c

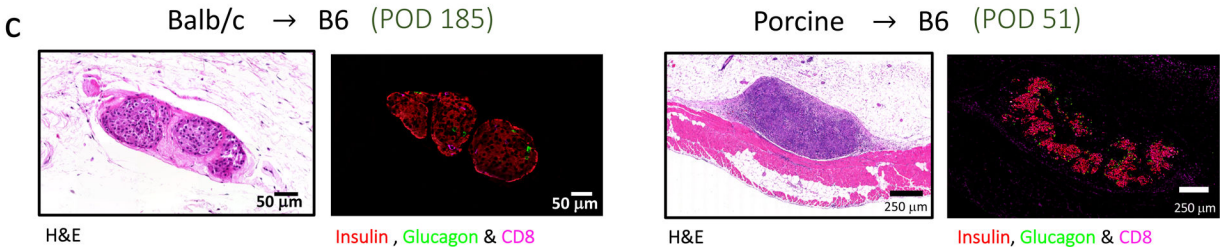

Figure 2.

Pancreatic islets transplanted in the subcutaneous space with IVM promote optimal glucose homeostasis in immune-competent recipients. **(a)** Immunotherapy regimen targeting T and B cell compartments to promote islet graft survival in immune-competent diabetic hosts. **(b)** The table shows survival data for islet allografts and xenografts transplanted subcutaneously in B6 mice. The days in the IVM^{+} group represent excision of the islet bearing skin at the times of elective retrieval and not due to destabilization of the grafts, unless the time is indicated by a$^{\phi}$ superscript. **(c)** H&E and IHC of islet bearing skin in long-term normoglycemic recipients of IVM^{+} islet grafts show abundant clusters of healthy α and β-cells.

a

Donor	Recipient	Number of islets	Graft	Islet graft survival in days (number of mice)
B6	B6	400	IA	Primary non-function ($n = 6$)
B6	B6	400	Islets + IVM	504 (×3), 482, 463(×2), 457(×2), 296(×2)
Porcine	B6/nude	500	IA	Primary non-function ($n = 4$)
Porcine	B6/nude	250	Islets + IVM	292(×3), 247(×3), 117(×2), 97(×3)
Porcine	B6/SCID	500	Islets + IVM	205 (×4)
Porcine	NOG	500	Islets + IVM	463 (×2), 151 (×4)
Porcine	NOG	250	Islets + IVM	122 (×4)
Human	B6/SCID	400	IA	Primary non-function ($n = 4$)
Human	B6/SCID	400	Islets + IVM	128 (×2), 62 (×2)

b

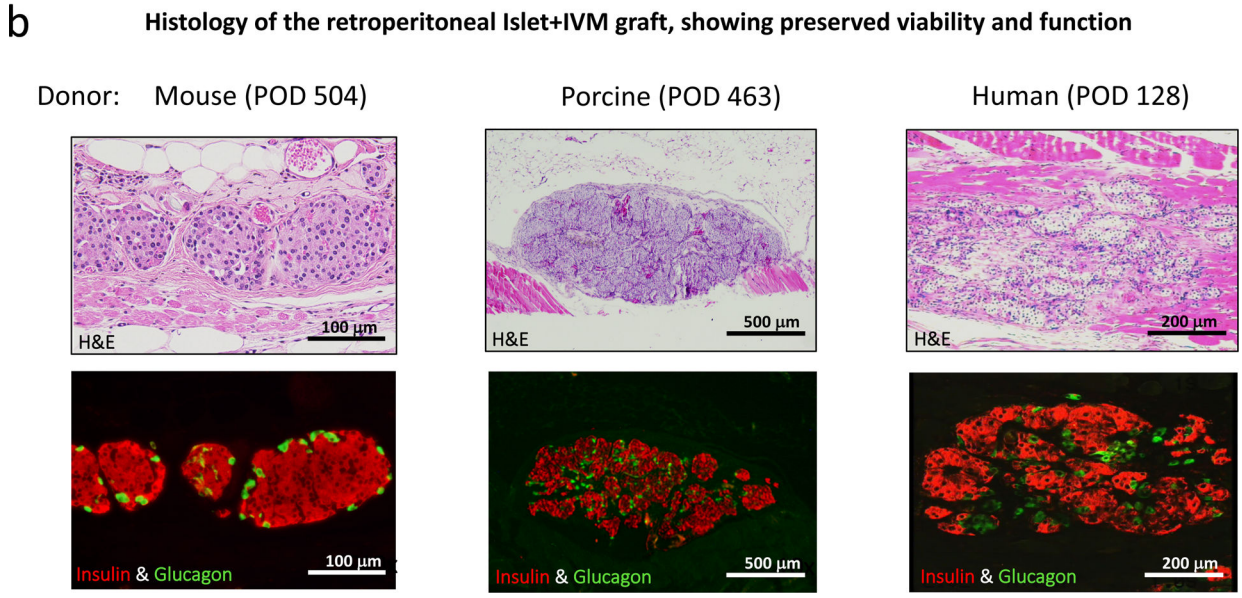

Figure 3.

The islet-IVM mixture of pancreatic islets transplanted in the retroperitoneal space renders the recipients normoglycemic. **(a)** Table demonstrating individual islet graft survival ± IVM in the retroperitoneal space of immunoincompetent diabetic mice for experiments utilizing mouse, pig or human islets. In all cases, the days in the IVM^+ group represent excision of the islet bearing skin at the times of elective retrieval and not due to destabilization of the grafts. Islets transplanted without IVM uniformly resulted in primary non-function. **(b)** β-cell morphology and endocrine function is maintained in retroperitoneal islet transplantation admixed with IVM. The top panels display H&E stains from murine, porcine and human grafts, displaying abundant viable cell clusters in the islets during long-term follow-up post-transplantation. In conjunction, the bottom panel substantiates the presence of insulin (red) and glucagon (green), correlating with the functional status of the grafted islets.

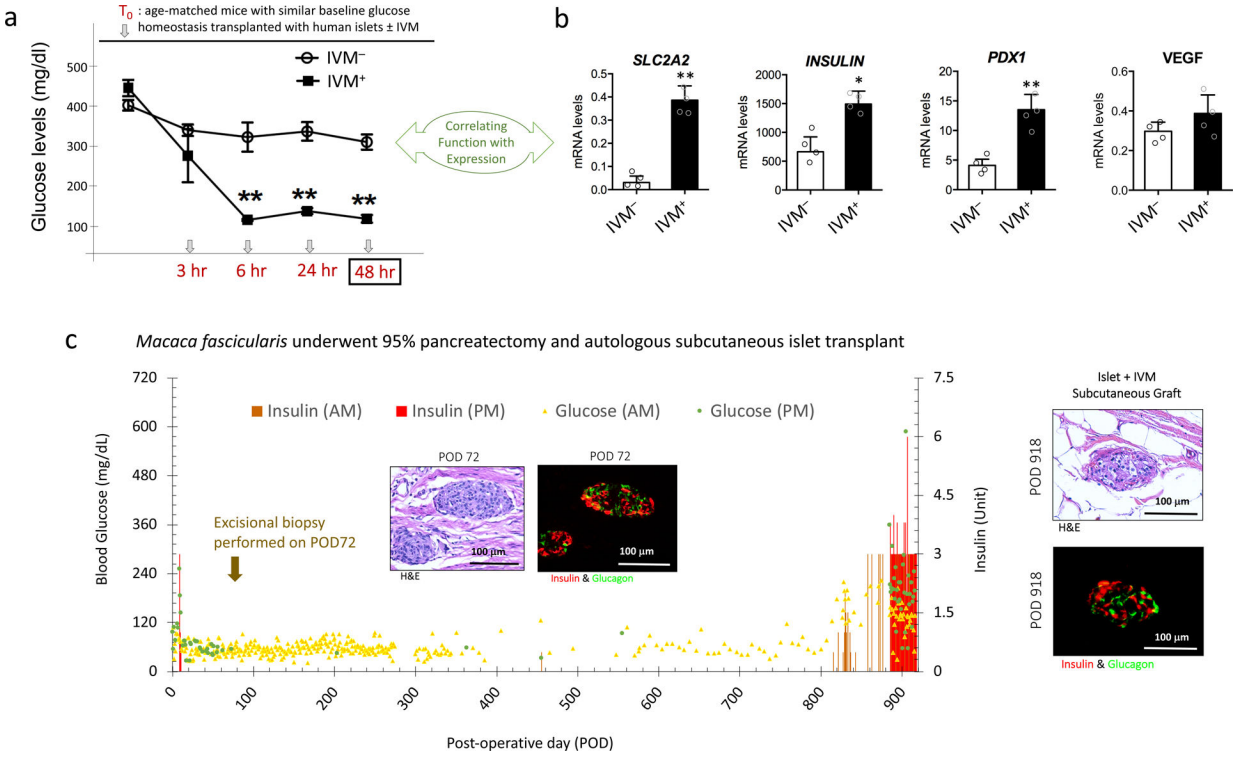

Figure 4.

IVM imparts enhanced viability to the subcutaneously transplanted human islets, as reflected in anti-apoptotic and pro-angiogenic signals. **(a)** Blood glucose levels of diabetic B6 SCID mice transplanted with 500 human islets ± IVM (n=4 animals in each group) showed that within 6 hours, animals in the IVM$^+$ cohort are rendered normoglycemic. Mean glycemic values for each experimental group are plotted, and the error bars represent the standard deviation. ** denotes p-values of 4×10^{-7}, 3×10^{-8} and 8×10^{-6} (at 6, 24 and 48 hours, respectively) between the IVM+ and IVM$^-$ group using the one-sided Mann-Whitney U Test. On POD 2, the grafts were excised to correlate gene expression with function. **(b)** Levels of SLC2A2 (p=0.002), INSULIN (p=0.01), PDX1 (p=0.003) and VEGF (p=0.43) in IVM$^-$ (white bars; n=4 mice) and IVM$^+$ (black bars; n=4 mice) islet groups were analyzed by RT-PCR; each dot represents an individual data point. Relative mRNA levels were normalized to HPRT and expressed as mean ± SEM (* denotes $p < 0.05$ and ** denotes $p < 0.005$ based on one-sided Student's t-test). **(c)** A Male cynomolgus monkey underwent ~90% pancreatectomy, and 5 hours later, underwent subcutaneous implantation of isolated islets with IVM. During this interval, glucose levels were elevated (>200 mg/dl) but remained in the normal range after auto-transplantation. On POD 72, a partial excisional biopsy was performed, demonstrating abundant clusters of islets with robust expression of insulin and glucagon. Longitudinal monitoring of blood glucose in this monkey revealed optimal glucose homeostasis until POD 820 when we observed progressive evidence of hyperglycemia mandating administration of exogenous insulin to the animal. As this monkey became overtly diabetic, per IACUC it was subjected to euthanasia on POD 918. Importantly, the histologic examination of the skin at the site of islet implantation

demonstrated persistence of well granulated islet endocrine clusters in the subcutaneous space without evidence of fibrosis and inflammatory cell infiltration.